

Supporting Information

A low-symmetry monothiatruxene-based hole transport material for planar n-i-p perovskite solar cells with 18.9% efficiency

Ellie Tanaka, ‡^a Gyu Min Kim, §^b Michał R Maciejczyk, ||^a Ayumi Ishii, ¶^b Gary S. Nichol,^a Tsutomu Miyasaka,^{*b} Neil Robertson ^{*a}

^a School of Chemistry, University of Edinburgh, Kings Buildings, Edinburgh EH9 3FJ, UK.

^b Graduate School of Engineering, Tooin University of Yokohama, 1614 Kuroganecho, Aoba, Yokohama, Kanagawa, 225-8503, Japan.

‡ Current address: Science & Innovation Center, Mitsubishi Chemical Corporation, 1000 Kamoshidacho, Aoba, Yokohama, Kanagawa, 227-8502, Japan.

§ Current address: Faculty of Food Biotechnology and Chemical Engineering, Hankyong National University, Anseong, Gyeonggi-Do, 17579, Republic of Korea.

|| Current address: Cambridge Display Technology Limited, Unit 12 Cardinal Park, Cardinal Way, Godmanchester, Cambridgeshire, PE29 2XG, UK.

¶ Current address: Faculty of Life and Environmental Sciences, Teikyo University of Science, 2525 Yatsusawa, Uenohara, Yamanashi, 409-0193, Japan.

Contents:

Experimental

Materials and Synthesis

Materials preparation

Synthesis of [1]-[8]

Solar cell fabrication and characterisation

Other materials/device characterisation

Preparation and characterisation of the TrxS-2Br single crystal by single X-ray diffraction

Preparation and characterisation of the TrxS-2MeOTAD single crystal by single X-ray diffraction

Fabrication and characterisation of the SCLC devices

UV/Vis absorption and photoluminescence measurements

Computational calculations

Cyclic voltammetry

Powder X-ray diffraction (PXRD)

Scanning electron microscopy (SEM)

Tables and Figures

Fig. S1 (a) Absorbance and emission of TrxS-2MeOTAD. (b) Photoluminescence of a TrxS-2MeOTAD thin film.

Table S1 Experimental values of thermal properties of TrxS-2MeOTAD.

Fig. S2 First heating profile of the differential scanning calorimetry (DSC).

Table S2 Full crystal parameters of TrxS-2Br and TrxS-2MeOTAD.

Fig. S3 PXRD patterns of TrxS-2MeOTAD in different forms.

Fig. S4 Time-resolved photoluminescence decay curves of Spiro-MeOTAD/perovskite and TrxS-2MeOTAD/perovskite films

Table S3 Fitted constants from the TRPL measurements.

Fig. S5 Statistical performance of PSCs with TrxS-2MeOTAD HTM spin-coated from solutions with HTM concentrations varying from 30 mM to 50 mM in chlorobenzene.

Fig. S6 Statistical performance of PSCs with TrxS-2MeOTAD HTM spin-coated from 40 mM solutions, with a varied ratio of HTM/LiTFSI. The HTM/LiTFSI molar ratio was set as 1:x, where x was varied from 0 to 0.55.

Fig. S7 (a) PXRD pattern of complete PSCs with TrxS-2MeOTAD or Spiro-MeOTAD HTM. Cross-section SEM image of a complete PSC with (b) TrxS-2MeOTAD and (c) Spiro-MeOTAD as HTM.

Fig. S8 SEM images of TrxS-2MeOTAD spin-coated onto FTO-glass without and with heating.

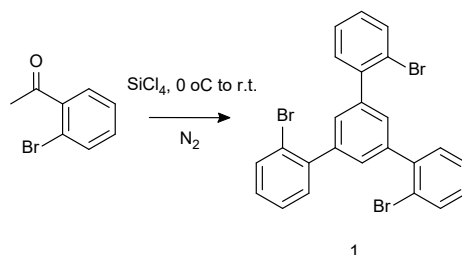
Experimental

Materials and Synthesis

Materials preparation

All materials were used as purchased without further purification. Materials for the synthesis of TrxS-2MeOTAD were purchased from Merck, Fluorochem, Fisher Scientific and VWR. The materials for the device fabrication were purchased from Wako, TCI, Merck and Alfa Aesar.

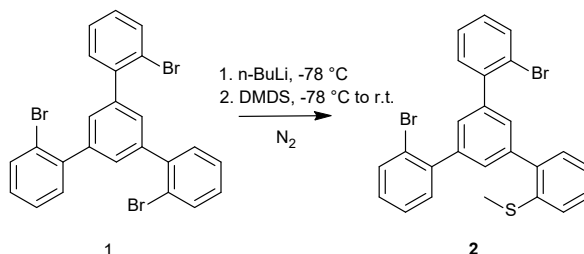
Synthesis of 1,3,5-tris-2'-bromophenylbenzene [1]



1,3,5-tris-2'-bromophenylbenzene was synthesised following the literature procedure.¹ SiCl₄ (33.0 g, 22.3 mL) was quickly added to 2'-bromoacetophenone (12.9 g, 8.7 mL) in anhydrous ethanol (100 mL) at 0°C under N₂. The resulting red solution was stirred at room temperature overnight under N₂. The mixture was quenched with water (250 mL) and the yellow precipitate was filtered off, washed with water, and recrystallised from hot ethanol. Drying in vacuum gave the product as a pale yellow solid (8.34 g, 71.2% yield).

¹H NMR (500 MHz, CDCl₃): δ 7.69 (dd, *J* = 8.0, 1.2 Hz, 3H), 7.50 (s, 3H), 7.46 (dd, *J* = 7.6, 1.7 Hz, 3H), 7.38 (td, *J* = 7.5, 1.3 Hz, 3H), 7.22 (ddd, *J* = 8.0, 7.3, 1.8 Hz, 3H).

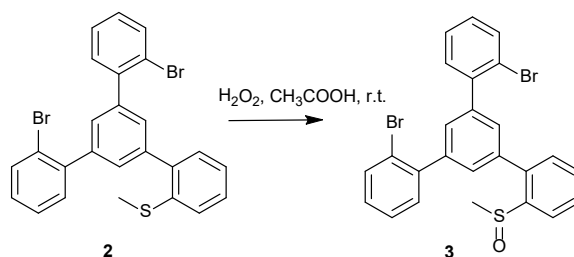
Synthesis of 1,3-bis(2-bromophenyl)-5-(2-thiomethylphenyl)benzene [2]



Compound [1] (5.00 g, 9.21 mmol) was dissolved in dry tetrahydrofuran (30 mL) under N₂. *n*-butyl lithium solution (2.5 M in hexanes, 3.84 mL, 9.60 mmol) was added dropwise at -78 °C. After 1h at this temperature, dimethyl disulphide (0.85 mL, 9.60 mmol) in 3.0 mL tetrahydrofuran was added, and the reaction was brought to r.t. and stirred overnight. Then it was quenched with saturated NH₄Cl and extracted with ethyl acetate. The organic layer is dried over MgSO₄ and filtered. The filtrate is evaporated to give a yellow brown oil (5.10 g). This crude product was used for the next reaction.

¹H NMR (500 MHz, CDCl₃): δ 7.72 – 7.66 (m, 2H), 7.56 – 7.42 (m, 5H), 7.35 (dddd, *J* = 11.8, 9.9, 6.5, 5.0, 3.3 Hz, 5H), 7.21 (qt, *J* = 7.5, 2.3 Hz, 3H), 2.40 (d, *J* = 6.8 Hz, 3H).

Synthesis of 1,3-bis(2-bromophenyl)-5-(2-oxothiophenyl)benzene [3]



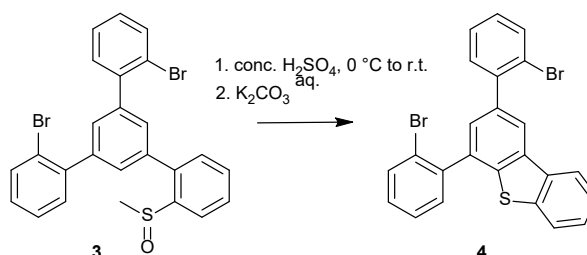
Crude compound **[2]** (5.10 g) was stirred vigorously in dichloromethane (2 mL), in which glacial acetic acid (30 mL) and H₂O₂ (30%, 1.4 mL) were added at room temperature. The reaction was stirred at r.t. overnight until the solution became clearer. The reaction was quenched with water and extracted with dichloromethane. The organic layer was washed with saturated Na₂CO₃ to remove the acid and was dried over MgSO₄. The solvent was removed by a rotary evaporator to give a light yellow foamy solid. Flash column chromatography of the crude product with hexane/acetone (5:1, v/v) yielded the product as a white foamy solid (3.25 g, 67.1% yield).

¹H NMR (500 MHz, CDCl₃): δ 8.18 – 8.12 (m, 1H), 7.72 – 7.37 (m, 12H), 7.25 – 7.21 (m, 2H), 2.49 (s, 3H).

¹³C NMR (126 MHz, CDCl₃): δ 144.30, 142.43, 141.87, 141.66, 141.64, 140.14, 139.16, 138.92, 138.28, 137.55, 133.40, 131.45, 131.36, 130.92, 130.88, 130.60, 130.56, 130.44, 129.42, 129.40, 129.13, 129.05, 128.20, 128.06, 127.71, 127.41, 127.38, 127.19, 123.67, 123.64, 122.71, 41.90, 41.77, 31.73, 22.80, 14.26.

MS (ESI): m/z (%) = Found: 524.95100 (found), calculated for C₂₅H₁₉Br₂OS (M⁺H) = 524.95179.

Synthesis of 1,3-bis(2-bromophenyl)-dibenzothiophene **[4]**

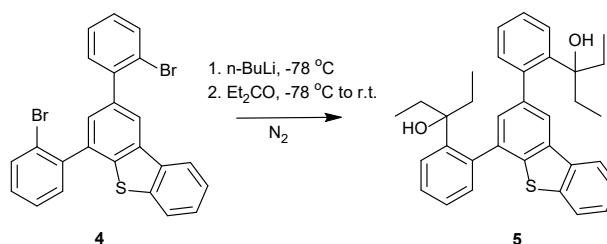


Compound **[3]** (3.07 g) was added in portions to stirred conc. H₂SO₄ 15 mL, in a one-neck round-bottom flask with a CaCl₂ guard tube at 0–5 °C. After stirring at r.t. for 1 h, the reaction was poured on ice-cold water (200 mL) and neutralised with K₂CO₃ aq. (pH 8). Then it was extracted with ethyl acetate and the organic layer was dried over Na₂SO₄, filtered and dried on a rotary evaporator to give a pale pink foamy solid. Flash column chromatography with hexane/ethyl acetate (30:1, v/v) gave the product as a white foamy solid (~2.39 g, 82.9% yield).

¹H NMR (500 MHz, CDCl₃): δ 8.23 (d, *J* = 1.7 Hz, 1H), 8.22 – 8.17 (m, 1H), 7.84 – 7.71 (m, 3H), 7.60 – 7.39 (m, 7H), 7.33 (ddd, *J* = 8.0, 7.4, 1.7 Hz, 1H), 7.25 (ddd, *J* = 8.1, 7.4, 1.8 Hz, 1H).

¹³C NMR (126 MHz, CDCl₃): δ 142.34, 141.08, 140.87, 140.22, 139.24, 138.23, 137.83, 135.93, 135.79, 135.69, 133.44, 133.40, 131.81, 131.18, 129.97, 129.30, 129.19, 129.08, 128.99, 128.49, 127.71, 127.64, 127.61, 127.55, 127.33, 127.12, 124.68, 123.41, 123.13, 122.98, 122.05, 121.86, 119.50, 60.54, 21.20, 14.36.

Synthesis of 1,3-bis(2-diethylhydroxymethylphenyl)-dibenzothiophene **[5]**



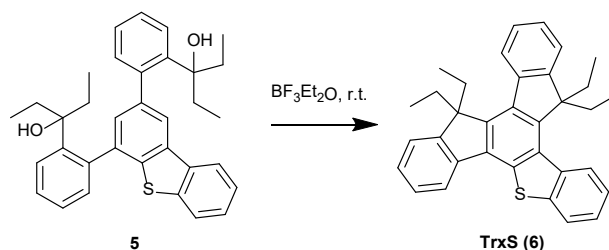
To a solution of compound **[4]** (1.00 g) in dry tetrahydrofuran (6 mL) under N₂, *n*-butyllithium solution (2.5 M in hexanes, 1.7 mL) was dropwise added at –78 °C. After 30 min at this temperature, 1.5 mL 3-pentanone/dry tetrahydrofuran (9:20, v/v) was injected. The reaction was slowly brought to r.t. and stirred overnight. Then it was quenched with saturated NH₄Cl aq. and extracted with ethyl acetate. The organic layer was dried over MgSO₄ and dried over a rotary evaporator to give a clear yellowish oil. Flash column chromatography with petroleum ether/ethyl acetate (10:1, v/v) yielded the product as a foamy white solid (0.490 g, 47.6% yield).

¹H NMR (500 MHz, CDCl₃) δ 8.14 – 8.06 (m, 1H), 7.95 (s, 1H), 7.81 – 7.75 (m, 1H), 7.44 (t, *J* = 4.8 Hz, 2H), 7.44 – 7.36 (m, 4H), 7.34 – 7.20 (m, 4H), 7.18 (d, *J* = 7.4 Hz, 1H), 2.03 – 1.92 (m, 2H), 1.89 – 1.75 (m, 1H), 1.77 – 1.71 (m, 1H), 1.61 – 1.48 (m, 1H), 1.39 – 1.24 (m, 1H), 1.21 (s, 1H), 1.15 (d, *J* = 12.3 Hz, 1H), 0.97 – 0.74 (m, 12H).

¹³C NMR (126 MHz, CDCl₃) ¹³C NMR (126 MHz, CDCl₃) δ 144.43, 140.62, 138.72, 138.48, 135.94, 132.58, 132.19, 128.08, 127.89, 127.45, 126.82, 126.27, 125.59, 124.47, 122.97, 121.97, 119.65, 80.25, 79.89, 40.99, 36.51, 36.13, 36.05, 35.54, 35.08, 33.98, 29.85, 28.58, 23.97, 20.93, 17.63, 17.44, 14.79, 8.64, 8.47, 8.35, 8.06.

MS (ESI⁺): m/z (%) = 531.23180 (found), 531.23282 (calculated for C₃₄H₃₆O₂NaS (M + ²³Na)).

Synthesis of Monothiatruxene [6]



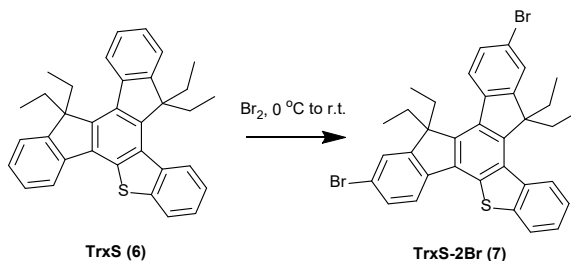
Compound [5] (0.38 g, 0.75 mmol) was dissolved in dichloromethane (8 mL) at r.t., where $\text{BF}_3\text{Et}_2\text{O}$ (0.3 mL, 2.4 mmol) was injected and stirred for 30 min. The reaction was quenched with methanol, concentrated on a rotary evaporator, and filtered and washed with methanol to give the product as a white solid (0.250 g, 70.8% yield).

^1H NMR (500 MHz, CDCl_3): δ 8.95 – 8.89 (m, 1H), 8.35 (dd, J = 7.1, 1.6 Hz, 1H), 8.17 (dt, J = 7.5, 0.9 Hz, 1H), 8.05 – 8.00 (m, 1H), 7.55 (ddd, J = 8.3, 7.1, 1.5 Hz, 1H), 7.55 – 7.47 (m, 4H), 7.47 – 7.37 (m, 3H), 3.12 (dq, J = 14.4, 7.2 Hz, 2H), 2.98 (dq, J = 14.5, 7.3 Hz, 2H), 2.33 – 2.22 (m, 4H), 0.24 (q, J = 7.2 Hz, 12H).

^{13}C NMR (126 MHz, CDCl_3): δ 152.24, 152.08, 146.03, 142.64, 140.96, 140.72, 140.48, 137.72, 135.97, 134.57, 133.00, 132.83, 127.20, 127.15, 127.11, 126.74, 126.56, 125.93, 124.20, 124.02, 123.32, 122.47, 122.17, 121.79, 58.93, 57.93, 29.95, 29.86, 29.65, 8.94, 8.89.

MS (ESI $^+$): m/z (%) = 651.03220 (found), 651.03272 (calculated for $\text{C}_{34}\text{H}_{30}\text{Br}_2\text{NaS}$ ($M + ^{23}\text{Na}$)).

Synthesis of dibromo-monothiatruxene (TrxS-2Br) [7]



TrxS (0.250g, 0.53 mmol) in DCM (10 mL) was cooled to 0°C. Br_2 (0.1 mL, 0.8 mmol) was added and slowly brought to r.t. After overnight stirring the reaction was quenched by sodium thiosulfate aq. After extraction with DCM and drying over sodium sulfate, the solvent was evaporated to give the product as a pale-yellow solid (0.330 g, 99.0%).

^1H NMR (500 MHz, CDCl_3) δ 8.91 – 8.85 (m, 1H, Ar-H), 8.17 (d, J = 8.4 Hz, 1H, Ar-H), 8.02 (d, J = 8.2 Hz, 2H, Ar-H), 7.67 – 7.60 (m, 3H, Ar-H), 7.60 – 7.49 (m, 3H, Ar-H), 3.12 (dq, J = 14.4, 7.2 Hz, 2H, CH_2), 2.89 (dq, J = 14.5, 7.3 Hz, 2H, CH_2), 2.24 (dp, J = 14.6, 7.1 Hz, 4H, CH_2), 0.25 (td, J = 7.3, 4.8 Hz, 12H, CH_3).

^{13}C NMR (126 MHz, CDCl_3) δ 154.60 (C_{Ar}), 154.18 (C_{Ar}), 146.10 (C_{Ar}), 142.15 (C_{Ar}), 140.28 (C_{Ar}), 139.76 (C_{Ar}), 139.44 (C_{Ar}), 136.62 (C_{Ar}), 135.18 (C_{Ar}), 134.20 (C_{Ar}), 133.47 (C_{Ar}), 132.98 (C_{Ar}), 130.37 (C_{Ar}), 129.98 (C_{Ar}), 129.83 (C_{Ar}), 127.14 (C_{Ar}), 126.28 (C_{Ar}), 125.77 (C_{Ar}), 125.59 (C_{Ar}), 125.21 (C_{Ar}), 124.48 (C_{Ar}), 123.40 (C_{Ar}), 123.14 (C_{Ar}), 121.48 (C_{Ar}), 121.15 (C_{Ar}), 59.18 ($\text{C}-(\text{CH}_2)_2$), 58.32 ($\text{C}-(\text{CH}_2)_2$), 29.92 (CH_2), 29.54 (CH_2), 8.91 (CH_3), 8.87 (CH_3).

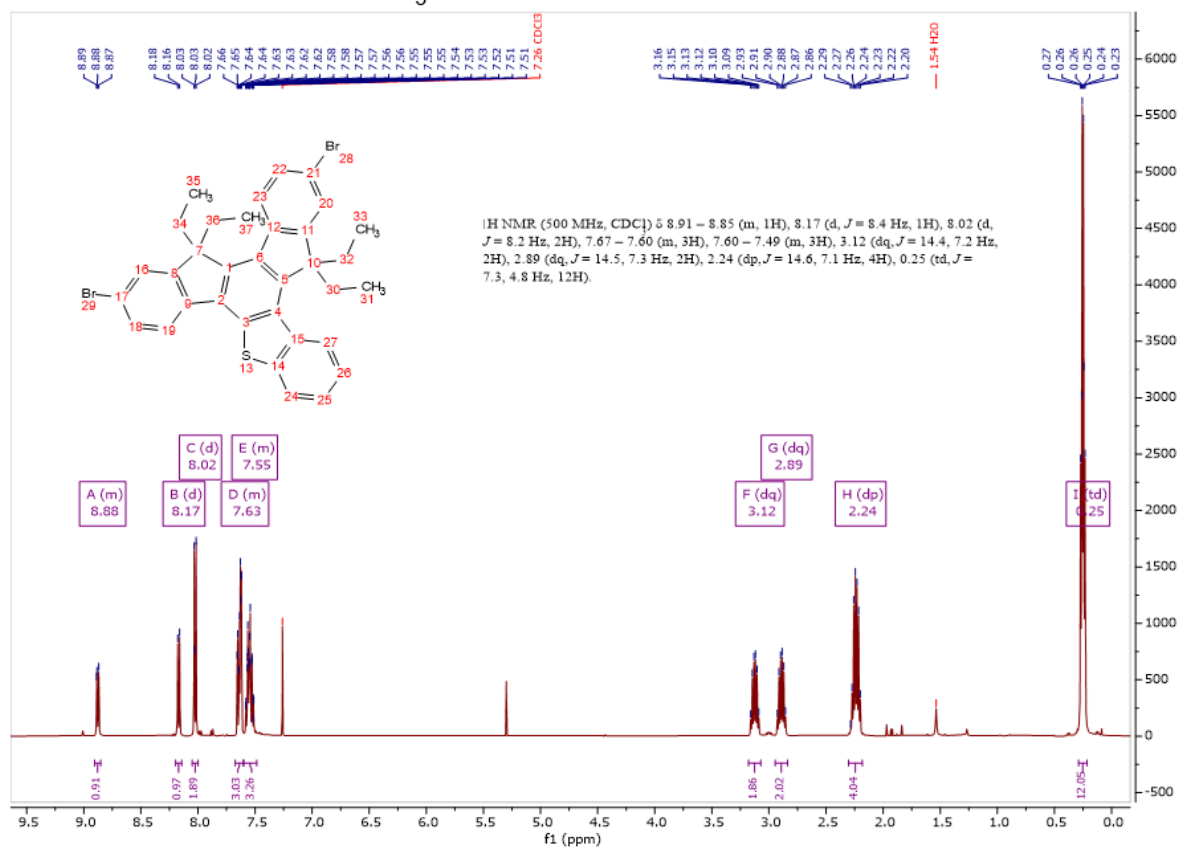
MS (ESI $^+$): m/z (%) = 651.03220 (found), 651.03272 (calculated for $\text{C}_{34}\text{H}_{30}\text{Br}_2\text{NaS}$ ($M + ^{23}\text{Na}$)).

Chemical reaction scheme showing the synthesis of **TrxS-2MeOTAD (8)** from **TrxS-2Br (7)**.

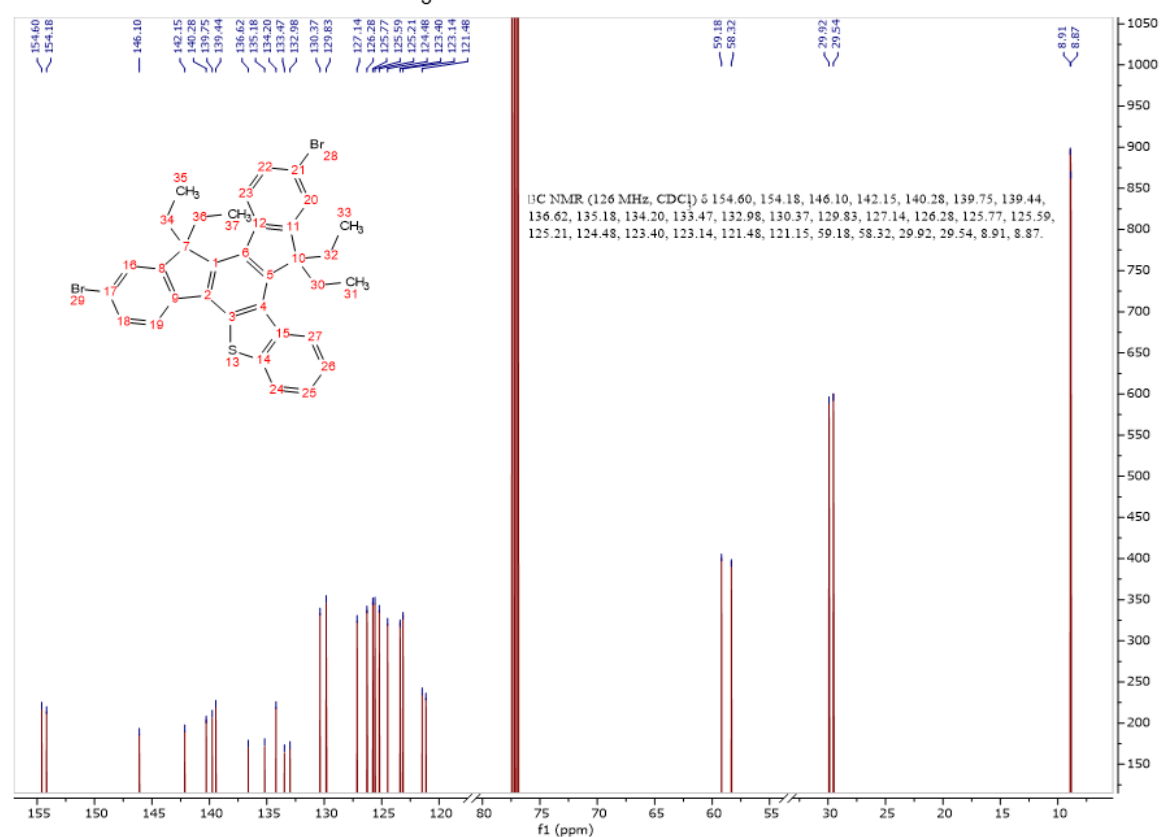
Reaction conditions: MeODPA , $\text{Pd}_2(\text{dba})_3$, $(\text{CH}_3)_3\text{CONa}$, $\text{P}(\text{tBu})_3$, N_2 , 110°C .

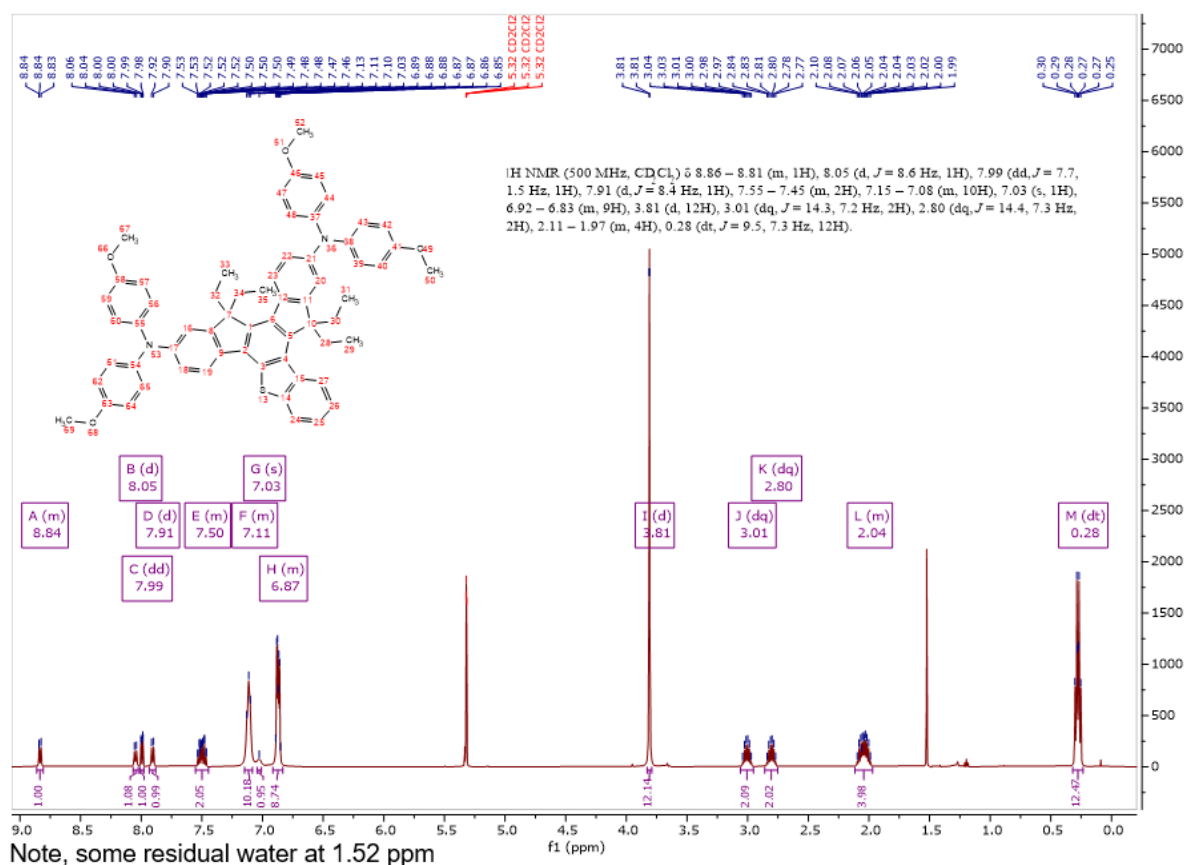
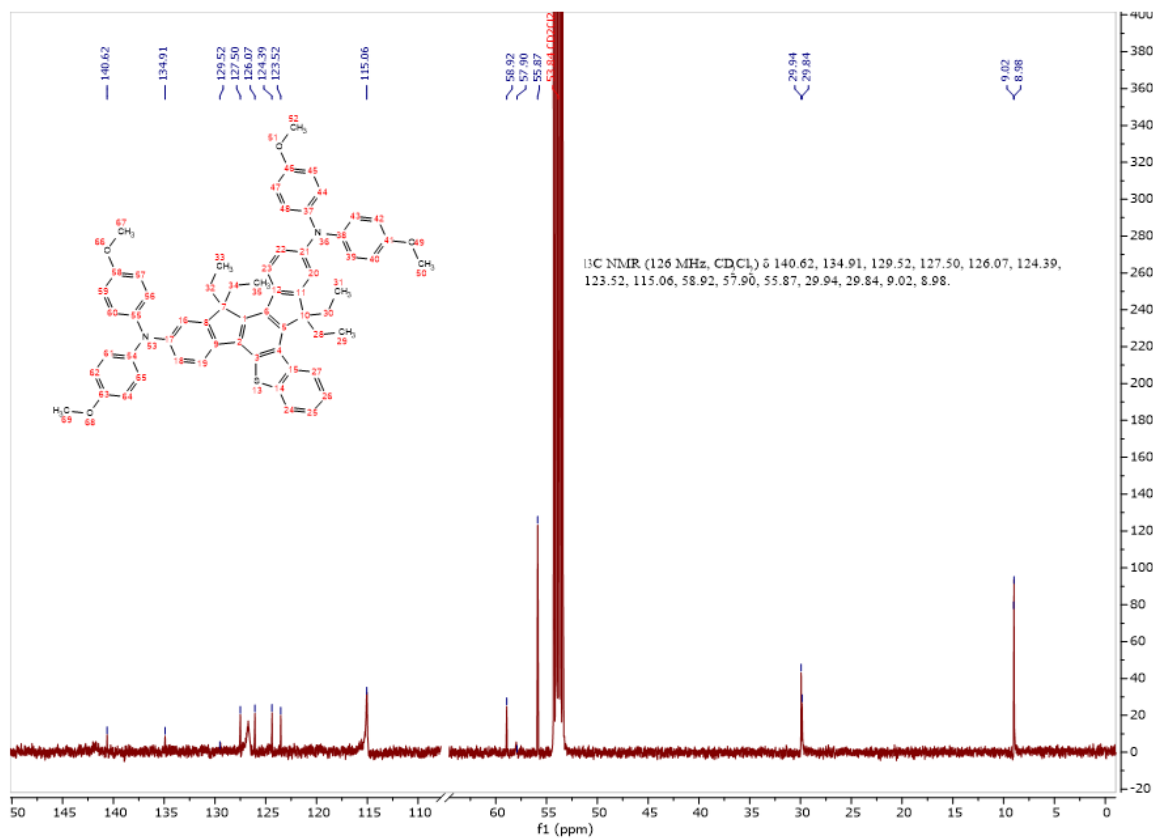
The reaction involves the coupling of two **TrxS-2Br (7)** units to form the dimeric product **TrxS-2MeOTAD (8)**, which features two **TrxS** units linked by a biaryl bond, each substituted with a 4-methoxyphenyl group.

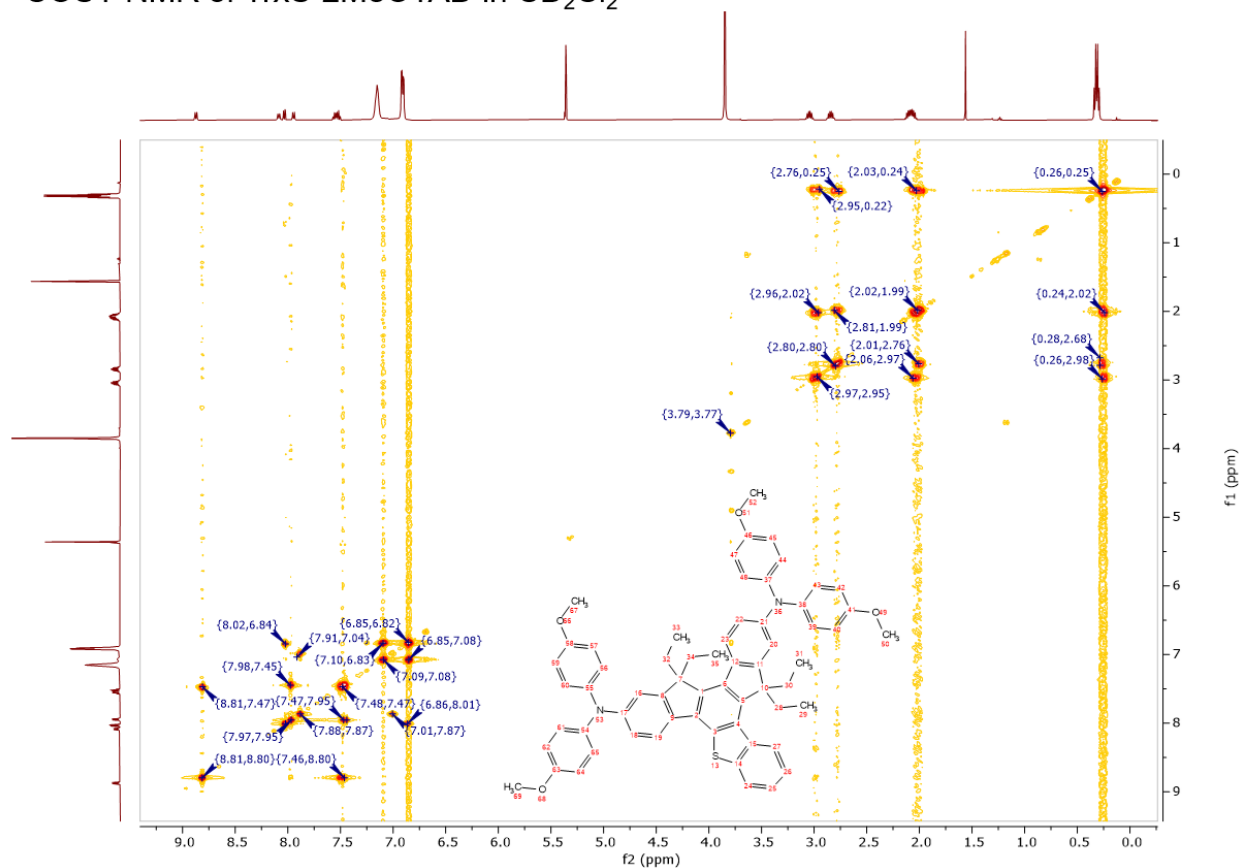
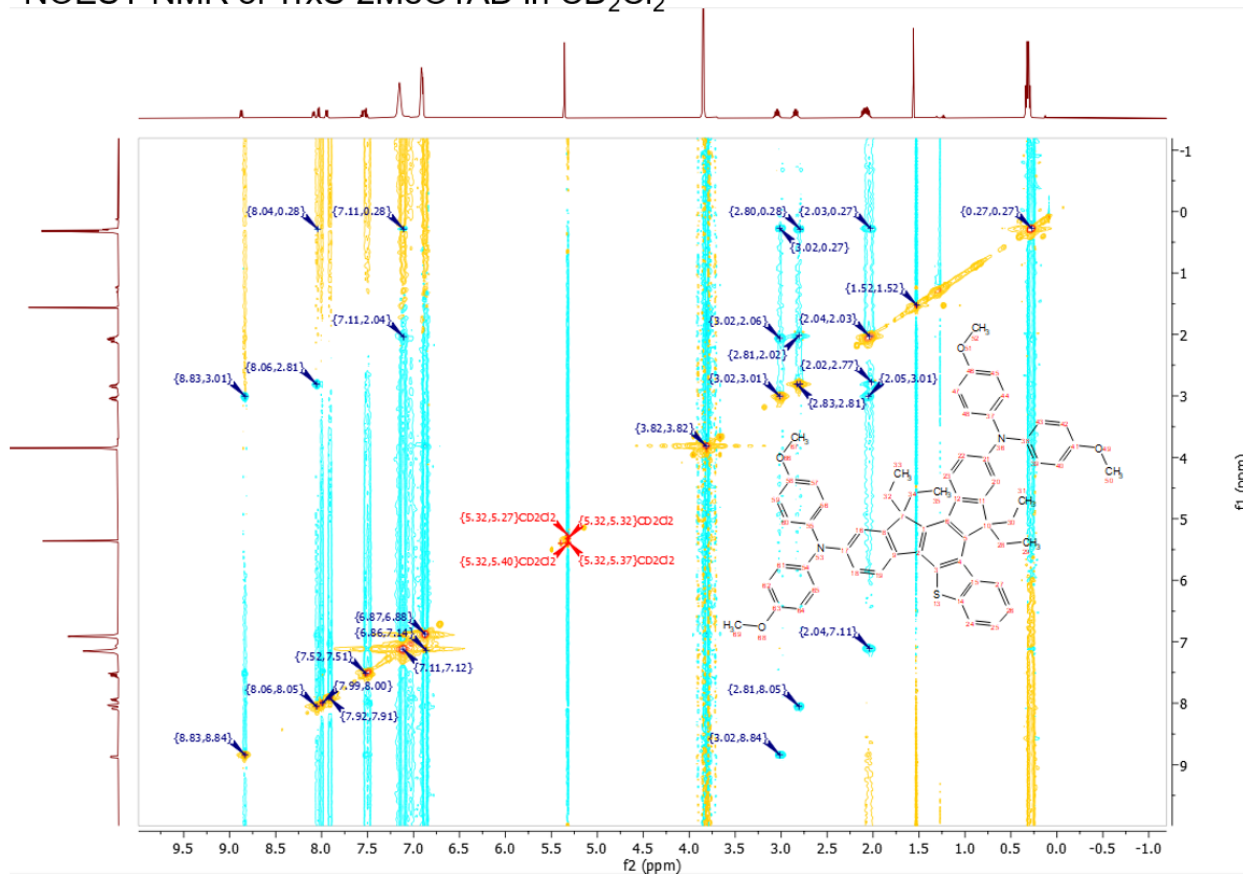
Please do not adjust margins

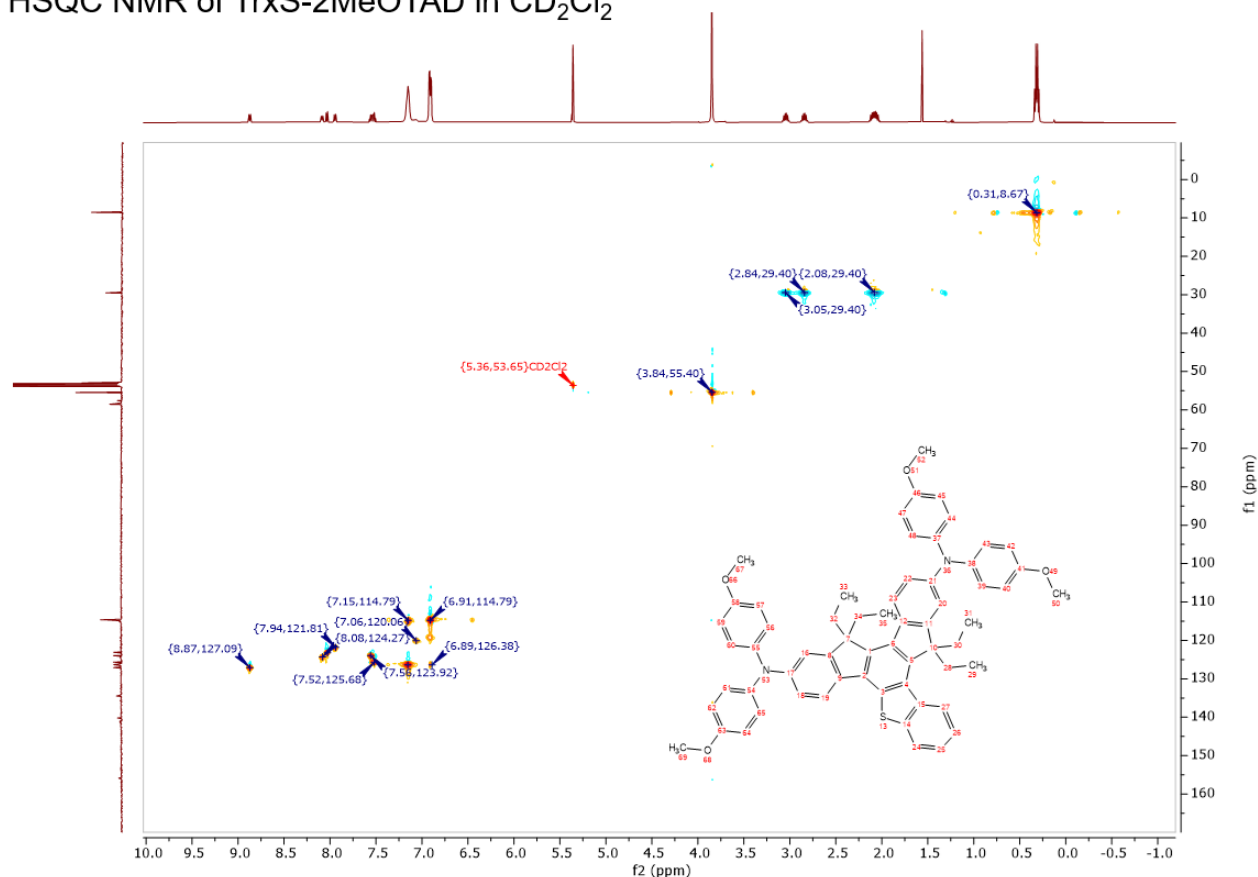
¹H NMR of TrxS-2Br in CDCl₃

Note, some residual DCM at 5.3 ppm

¹³C NMR of TrxS-2Br in CDCl₃

¹H NMR of TrxS-2MeOTAD in CD₂Cl₂¹³C NMR of TrxS-2MeOTAD in CD₂Cl₂

COSY NMR of TrxS-2MeOTAD in CD_2Cl_2 NOESY NMR of TrxS-2MeOTAD in CD_2Cl_2 

HSQC NMR of TrxS-2MeOTAD in CD₂Cl₂

Solar cell fabrication and characterization

The perovskite solar cells in this study were planar-type, with an architecture of FTO/c-TiO₂/c-SiO₂/(Cs_{0.04}FA_{0.80}MA_{0.16})Pb(I_{0.95}Br_{0.05})₃ perovskite/HTM/Au, where c-TiO₂ = compact TiO₂, c-SnO₂ = compact SnO₂, FA = formamidinium and MA = methyl ammonium.

Photoanodes. Fluorine-doped tin oxide (FTO) conductive glass (Pecell, 11 Ω/sq) was cut into 2.5 cm x 2.5 cm square pieces and cleaned by sonication in a 2% aqueous detergent solution (Hellmanex, Hellma), acetone, and then isopropanol for 20-30 min each. The substrates were dried with nitrogen flow and treated by UV/O₃ for 10 min. Titanium diisopropoxide bis(acetylacetonate) solution (commercial solution of 75 wt.% in isopropanol, mixed with anhydrous isopropanol at 1:9, v/v) was spin-coated on the substrates at 3000 rpm for 25 s, followed by drying at 100 °C for 1 min and further annealing at 500 °C for 30 min on a hotplate in ambient air. SnO₂ solution (commercial solution of 15 wt.% in H₂O, mixed with deionised water at 1:7, v/v) was spin-coated on the films pre-treated with UV/O₃ for 10 min at 5000 rpm for 25 s followed by drying at 160 °C for 15 min on a hotplate. After UV/O₃ treatment of the films for 2 min, the perovskite solution was spin-coated at 3000 rpm for 10 s followed by 5000 rpm 20 s, where 160 μL chlorobenzene was gently added at 8-10 s once 5000 rpm was reached. The perovskite solution consisted of methyl ammonium bromide 0.250 M, formamidinium iodide 1.25 M, PbI₂ 1.56 M and CsI 0.075 M (from 1.5 M CsI/DMSO stock solution) in dimethylformamide/dimethyl sulfoxide (3:1, v/v). After annealing at 110 °C for 15 min on a hotplate, the films were set aside to cool to r.t.. before the deposition of the HTM. The optimised HTM solution consisted of TrxS-2MeOTAD 37.0 mg (40 mM), lithium bis(trifluoromethanesulfonyl) imide (LiTFSI) solution (340 mg/mL MeCN) 14.7 μL, and *tert*-butyl pyridine (tBP) 19.7 μL in 1 mL of chlorobenzene for the TrxS-2MeOTAD, and Spiro-MeOTAD 72.3 mg (60 mM), LiTFSI (340 mg/mL MeCN stock) 26.8 μL and tBP 28.8 μL in 1 mL of chlorobenzene for the Spiro-MeOTAD. The HTM solution was spin-coated at 3000 rpm for 30 s, where the solution was dynamically deposited during the acceleration of 5 s. The films were left to oxidise at this stage (only if necessary) for a couple of hours in ambient air. Finally, ~50 nm of gold was deposited as the cathode by thermal evaporation in a vacuum chamber (SVC-700TM SG, Sanyu Electron) and a silver alloy (Cerasolzer Eco #155, Kuroda Techno) was applied to the anode after the redundant parts of the film were scraped off.

Photocurrent density-voltage (J - V) curves were recorded with a 2400 SourceMeter (Keithley) equipped with a class A solar simulator (PEC-L01, Peccell) as light source. The light intensity was calibrated to AM1.5G, 100 mW·cm⁻² using a reference silicon photodiode. The J - V scans were run with a step voltage of 0.01 V and settling time of 0.1 s, giving a scan rate of 0.1 V·s⁻¹. The solar cells were masked with an aperture of 0.090 cm².

The incident photon-to-current conversion efficiency (IPCE) was recorded with a PEC-S20 system in DC mode. The incident light was calibrated with a reference silicon photodiode within the range of 350 nm to 900 nm.

The operational stability measurement was performed as follows. The best-performing unencapsulated solar cell was selected, and the voltage at the maximum power point (V_{m0}) was detected by a normal J - V scan. Subsequently, the solar cell was kept at V_{m0} under constant illumination at AM1.5G, 100 mW·cm⁻² in ambient air for c.a. 4000 s (Stability assessment protocol ISOS-L-1).² The photocurrent at V_{m0} was plotted by the Peccell software, and the PCE values ($J \times V_{m0}$) were normalised based on the photocurrent attained in the stabilised region (= "initial" photocurrent).

Other materials/device characterisation

Preparation and characterization of the TrxS-2Br single crystal by single X-ray diffraction

Single colourless plate crystals were recrystallised from a mixture of ethanol and dichloromethane by solvent layering. A suitable crystal (0.51 × 0.18 × 0.03) mm³ was selected and mounted on a MITIGEN holder in Paratone oil on a Rigaku Oxford Diffraction SuperNova diffractometer. The crystal was kept at 120.0 K during data collection. Using Olex2 as the graphical interface,³ the structure was solved with the ShelXT 2018/2 solution programme using dual methods.⁴ The model was refined with ShelXL 2018/3 using full matrix least squares minimisation on F^2 .⁵

Preparation and characterization of the TrxS-2MeOTAD single crystal by single X-ray diffraction

Single colourless needle crystals were recrystallised from a mixture of ethanol and dichloromethane by solvent layering. A suitable crystal (0.08 × 0.05 × 0.01) mm³ was mounted on a MITIGEN holder in perfluoroether oil on a Diamond Light Source I-19 EH1 diffractometer.⁶ The crystal was kept at $T = 100.0$ K during data collection. The structure was solved using Olex2 as the graphical interface and with the ShelXS solution programme using direct methods.⁷ The model was refined with ShelXL 2018/3 using full matrix least squares minimisation on F^2 .

Fabrication and characterisation of the SCLC devices

For the space charge limiting current (SCLC) measurement, the device structure was ITO/PEDOT:PSS/HTM/Au, where ITO glass = indium tin oxide conductive glass and PEDOT:PSS = poly(3,4-ethylenedioxythiophene) polystyrene sulfonate. ITO glass (Flat ITO, Geomatec, 10 Ω/sq) was cleaned by sonication in isopropanol/water (3:1, v/v) and acetone for 15 min each. After UV/O₃ treatment of the substrates for 10 min, PEDOT:PSS solution (commercial solution of 1.5 wt.% in H₂O, Al 4083, Ossila) was spin-coated at 5000 rpm for 35 s. The films were subsequently dried at 150 °C for 15 min on a hotplate. Finally, the HTM layer was deposited by spin-coating without any prior treatment. The detailed procedure for the HTM deposition follows that of the solar cells. Dark J - V curves were recorded within an applied voltage range of -0.5 V to 4.0 V. The step voltage and settling time were 0.01 V and 0.1 s, respectively.

UV/Vis absorption and photoluminescence measurements

UV/Vis and steady-state photoluminescence (PL) profiles of the TrxS-2MeOTAD, in solution and as a film, were recorded on a UV-1800 (Shimadzu) spectrophotometer. TrxS-2MeOTAD powder was dissolved in dichloromethane at a concentration of 2.5·10⁻⁵ M and was placed in a quartz cell ($d = 1$ cm). For the film measurements, thin films of TrxS-2MeOTAD were spin-coated on quartz glass substrates from a 60 mM anhydrous chlorobenzene solution at 3000 rpm for 25 s. Dichloromethane and bare glass were selected as the background for the solution and film measurements, respectively.

Devices for steady-state PL and time-resolved PL had the architecture of glass/perovskite or glass/perovskite/HTM. The perovskite and HTM layers were deposited following the same procedure as for the solar cells. UV-Vis absorption was recorded on a UV-1800 (Shimadzu) spectrophotometer.

Steady-state PL measurements were performed on a Quantaauras-QY Plus C13534 (Hamamatsu Photonics) spectrophotometer. The excitation wavelength was set at 390 nm. TRPL decays were recorded on a Quantaauras-Tau C11367 (Hamamatsu Photonics) fluorescence lifetime spectrometer equipped with a C10196 (Hamamatsu Photonics) picosecond light pulser. A cut filter at 495 nm and neutral density filter were used. The emission peak was set at 780 nm.

Computational calculations

Density functional theory (DFT) based computational calculations were performed on a Gaussian09 package. The molecular orbitals were analysed by the Avogadro software. The calculations were based on the hybrid B3LYP functional with 6-311G(d) basis

set for elements H, C, O, S and N. Solution phase calculations were performed following the same procedure as the gas phase calculations, where dichloromethane was set as the solvent.

Cyclic voltammetry

A three-electrode, single compartment cell was used. The analyte was dissolved in 0.1M tetrabutylammonium hexafluorophosphate (TBAPF₆) in anhydrous dichloromethane. The working electrode was a Pt disc and the counter electrode was a Pt wire. The reference electrode was Ag/AgCl. The cyclic voltammetry (CV) scans were recorded on an Autolab potentiostat (Metrohm) with GPES software with scan rates from 0.05 V·s⁻¹ to 0.7 V·s⁻¹. Square wave voltammetry (SWV) was performed at a scan rate of 0.05 V s⁻¹. The potential vs. Ag/AgCl was calibrated with ferrocene after the measurement to derive the potential vs. normal hydrogen electrode (NHE).

Powder X-ray diffraction (PXRD)

X-ray powder diffraction (PXRD) was measured on a D8 Discover (Bruker) diffractometer, with CuK α radiation source at 40 kV and 50 mA. The samples were recorded with an increment of 0.02° per step.

Scanning electron microscopy (SEM)

SEM images were captured on an FE-SEM SU8000 (Hitachi) microscope with an acceleration voltage at 10.0 kV.

Tables and Figures

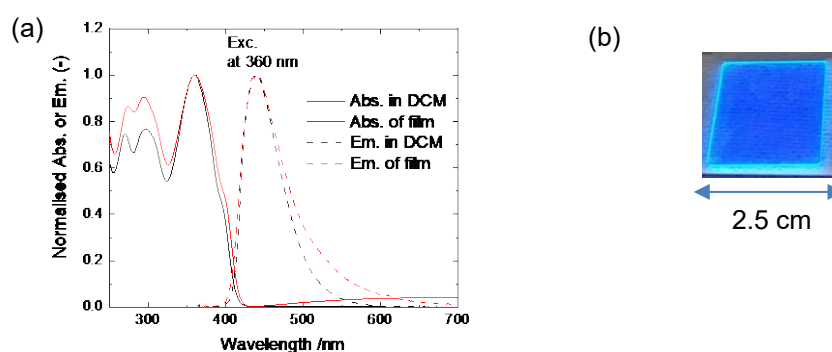


Fig. S1 (a) Absorbance (Abs.) and emission (Em.) of TrxS-2MeOTAD, dissolved in dichloromethane and as a thin-film. (b) Photoluminescence of a TrxS-2MeOTAD thin-film spin-coated on quartz glass, illuminated at 365 nm UV light.

TrxS-2MeOTAD in DCM and as a film show bright blue emission under UV light. An optical gap of 3.02 eV was derived from the intersection of the absorption/emission spectra (410 nm) in **Fig. S1 (a)**. This is slightly narrower than the calculated value of 3.49 eV but is in a suitable range. The LUMO was estimated as the sum of the HOMO and optical gap, hence ignoring any exciton binding energy. **Fig. S1(b)** is a photograph of a TrxS-2MeOTAD film excited at 365 nm. External photoluminescence quantum yields (PLQY) were derived from the steady-state photoluminescence (PL) measurements, resulting in a relatively high PLQY of 27.5% for the solution, and 6.3% for the film. The PLQY in solution is comparable to the monothiatruxene compounds reported as light-emitting materials by Maciejczyk et al.⁸

Table S1 Experimental values of thermal properties of TrxS-2MeOTAD. Literature data for Spiro-MeOTAD are shown as a reference.

HTM	$T_g / ^\circ\text{C}^a$	$T_m^1 / ^\circ\text{C}^b$	$T_m^2 / ^\circ\text{C}^c$	$T_d^{\text{on}} / ^\circ\text{C}^d$	$T_d^{0.5} / ^\circ\text{C}^e$	$T_d / ^\circ\text{C}^f$	$T_{\text{exo}} / ^\circ\text{C}^g$
TrxS-2MeOTAD	145	223 (221)	260 (261)	333	>400	447	463
Spiro-MeOTAD ^h	122	164	249	-	>360	-	-

^a Glass transition temperature, which was derived from the selected start point and extrapolated onset as shown in Fig. 5(b). ^b First melting point from TG-DTA and DSC (in parentheses). ^c Second melting point from TG-DTA and DSC (in parentheses). ^d Onset of decomposition. ^e Temperature at 0.5% weight loss. ^f Intersect of baseline and linear slope of decomposition step. ^g Exothermic peak temperature. ^h Values taken from the literature and Ossila website.^{9,10}

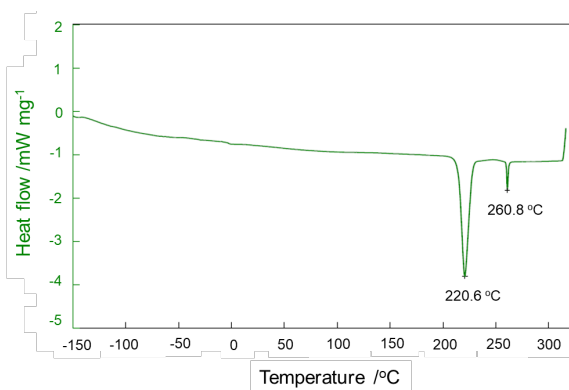


Fig. S2 First heating profile of the differential scanning calorimetry (DSC).

Table S2 Full crystal parameters of TrxS-2Br (CCDC 2235428) and TrxS-2MeOTAD (CCDC 2235429).

Compound name	TrxS-2Br	TrxS-2MeOTAD
Formula	$\text{C}_{34}\text{H}_{29.96}\text{Br}_{2.04}\text{S}$	$\text{C}_{63}\text{Cl}_2\text{H}_{60}\text{N}_2\text{O}_4\text{S}$
$D_{\text{calc.}} / \text{g cm}^{-3}$	1.551	1.287
μ / mm^{-1}	3.147	0.200
Formula Weight	633.61	1012.09
Colour	colourless	colourless
Shape	plate	needle
Size/ mm^3	$0.51 \times 0.18 \times 0.03$	$0.08 \times 0.05 \times 0.01$
T / K	120.01(10)	100.0

Journal Name	ARTICLE	
Crystal System	triclinic	monoclinic
Space Group	$P-1$	$P2_1/c$
$a/\text{\AA}$	7.3239(2)	17.771(3)
$b/\text{\AA}$	9.5641(4)	25.909(4)
$c/\text{\AA}$	20.1031(8)	11.8177(17)
$\alpha/^\circ$	77.186(3)	90
$\beta/^\circ$	84.695(3)	106.224(3)
$\gamma/^\circ$	81.803(3)	90
$V/\text{\AA}^3$	1356.35(9)	5224.6(13)
Z	2	4
Z'	1	1
Wavelength/ \AA	0.71073	0.6889
Radiation type	Mo K_α	Synchrotron
$\vartheta_{\min}/^\circ$	3.336	1.157
$\vartheta_{\max}/^\circ$	28.280	16.770
Measured Refl.	23435	25408
Independent Refl.	6479	3183
Reflections Used	4928	2347
R_{int}	0.0594	0.0972
Parameters	348	630
Restraints	0	588
Largest Peak	1.241	0.246
Deepest Hole	-0.867	-0.277
GooF	1.109	1.054
wR_2 (all data)	0.1102	0.2544
(Table continues below)		
(Continued from above)		
wR_2	0.1001	0.2415
R_1 (all data)	0.0845	0.1085
R_1	0.0542	0.0889

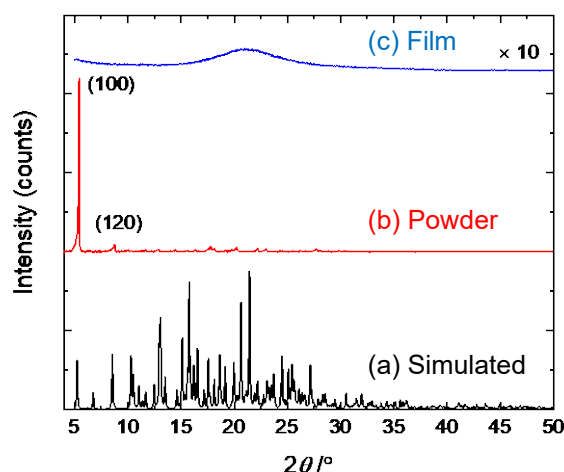


Fig. S3 PXRD patterns of TrxS-2MeOTAD in different forms: (a) simulated pattern from the SXRD analysis; (b) PXRD pattern of ground powder; (c) PXRD pattern of a spin-coated film on a microscope glass slide. The broad peak observed in the film pattern (10-times magnified) is the instrumental background peak. The numbers in brackets are the miller indices for the main peaks observed in (b).

The TRPL decay curves were interpreted as being composed of short-lived species and long-lived species. They were fitted with a double exponential equation:

$$y = Ae^{\left(\frac{-x_1}{\tau_1}\right)} + Be^{\left(\frac{-x_2}{\tau_2}\right)}, \quad (\text{Equation 2})$$

where A and B are constants, x_1 and x_2 are the time variables and τ_1 and τ_2 are the charge carrier lifetimes. The constants from the fittings are summarised in **Table 5**. The short-lived species in the perovskite-only film have a lifetime of 3.6 ns, where the long-lived species linger for more than 200 ns. When Spiro-MeOTAD is deposited on the perovskite, both short-lived and long-lived species are immediately quenched, making it impossible to derive a meaningful lifetime value (the decay times are shorter than the IRF). For the TrxS-2MeOTAD, the short-lived species are immediately quenched, whereas the long-lived species appear to reside for a few seconds longer than for the case of Spiro-MeOTAD. Nonetheless, the negligible differences confirm that both TrxS-2MeOTAD and Spiro-MeOTAD are highly efficient hole extractors.

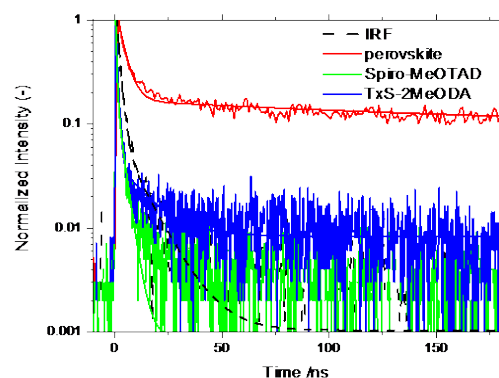


Fig. S4 Time-resolved photoluminescence decay curves of Spiro-MeOTAD/perovskite and TrxS-2MeOTAD/perovskite films.

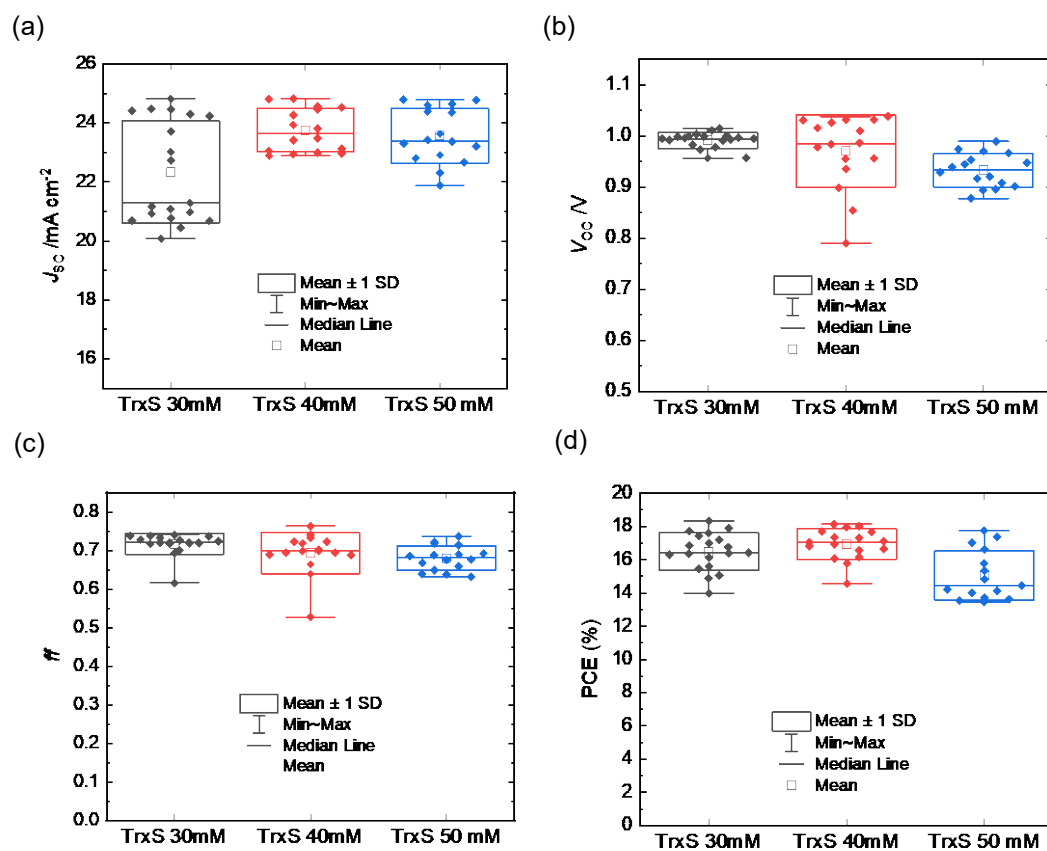


Fig. S5 Statistical performance of PSCs with TrxS-2MeOTAD HTM spin-coated from solutions with HTM concentrations varying from 30 mM to 50 mM in chlorobenzene. 40 mM was selected as the optimal concentration due to the highest average PCE attained.

Table S3 Fitted constants from the TRPL measurements.

Condition	A	τ_1 /s	B	τ_2 /s
Perovskite	1.32	3.58	0.088	214
Pero/Spiro-MeOTAD	1.90	0.50	0.21	2.97
Pero/TrxS-2MeOTAD	1.65	0.84	0.038	13.2
IRF	1.77	1.56	0.082	10.7

IRF: Instrument response function. Perovskite = <Glass/perovskite>. Pero/Spiro-MeOTAD = <Glass/perovskite/Spiro-MeOTAD>. Pero/TrxS-2MeOTAD = <Glass/perovskite/TrxS-2MeOTAD>.

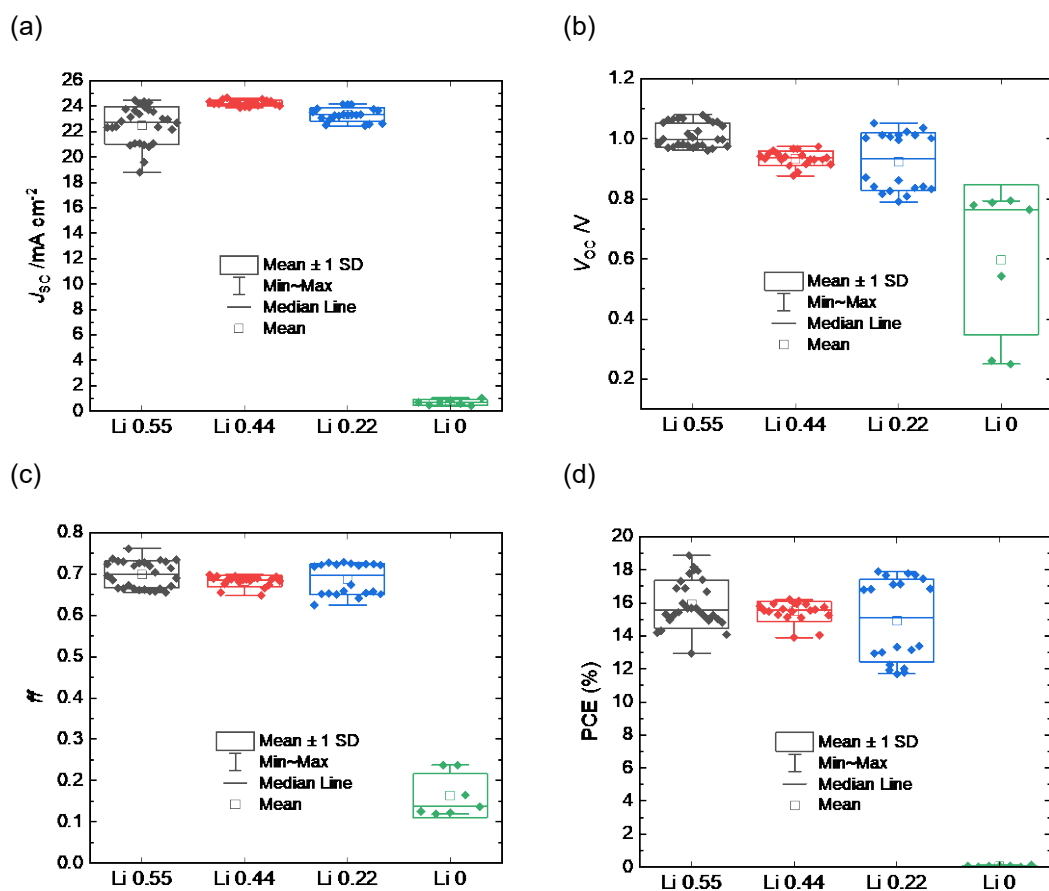


Fig. S6 Statistical performance of PSCs with TrxS-2MeOTAD HTM spin-coated from 40 mM solutions, with a varied ratio of HTM/LiTFSl. The HTM/LiTFSl molar ratio was set as 1:x, where x was varied from 0 to 0.55. The HTM/tBP ratio was fixed to 1:3.3 (mol/mol) for all conditions. In the figure, the HTM/LiTFSl ratio of 1:x is denoted as "Li x." The best PCEs were obtained with "Li 0.55."

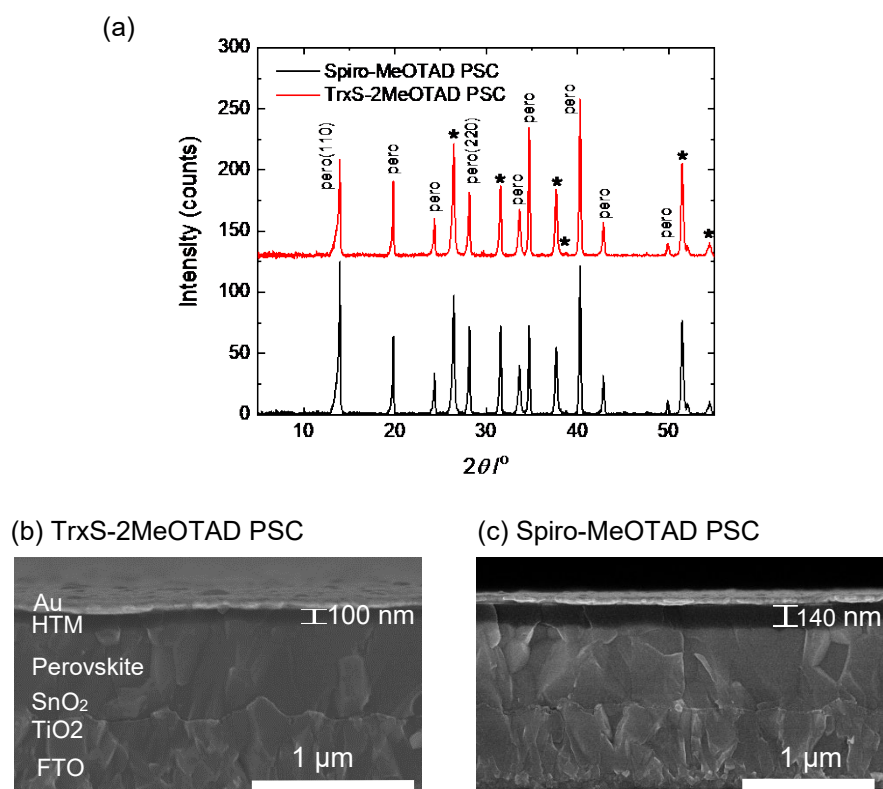
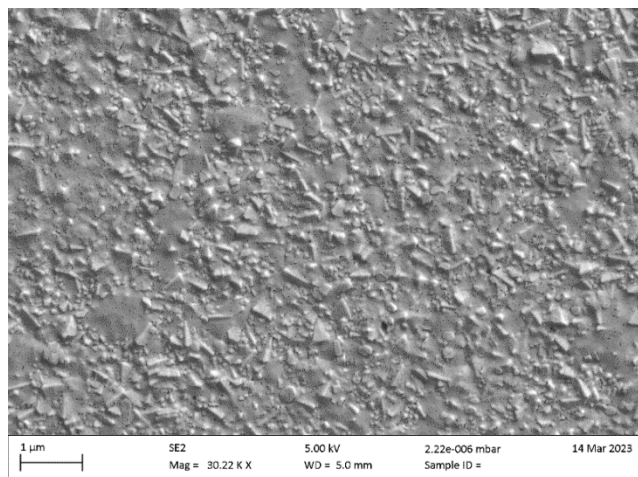
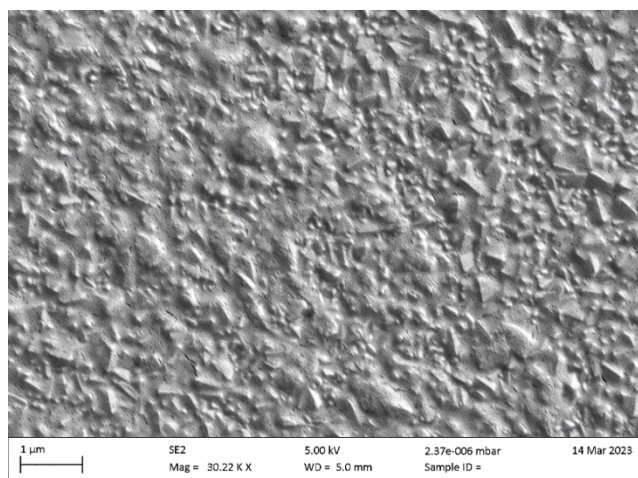


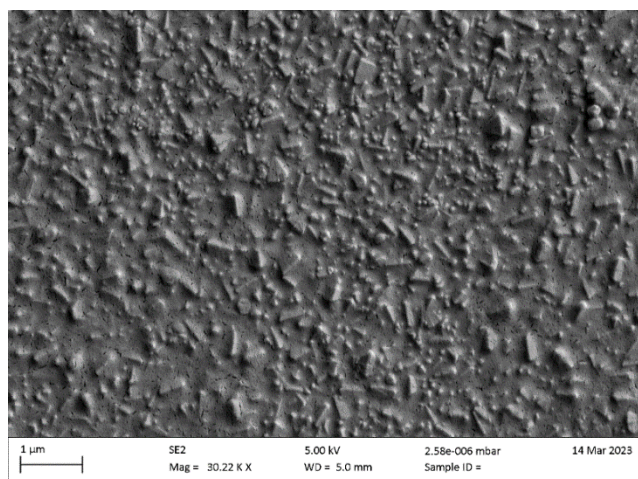
Fig. S7 (a) PXRD pattern of complete PSCs with TrxS-2MeOTAD or Spiro-MeOTAD HTM. The area without gold and silver-alloy electrodes is detected. The commonly discussed peaks for the perovskite are marked as “pero(miller index).” The other peaks associated to the perovskite are marked as “pero.” The asterisks (*) indicate the FTO substrate. Cross-section SEM image of a complete PSC with (b) TrxS-2MeOTAD and (c) Spiro-MeOTAD as HTM. The scale bar is 1 μm .



Not Heated



10 mins at 135 °C



10 mins at 155 °C

Fig. S8 Scanning electron microscope images of TrxS-2MeOTAD spin coated onto FTO-glass without and with heating.

References

- 1 D. Trawny, M. Quennet, N. Rades, D. Lentz, B. Paulus and H. Reissig, *European J. Org. Chem.*, 2015, 4667–4674.
- 2 M. V. Khenkin, E. A. Katz, A. Abate, G. Bardizza, J. J. Berry, C. Brabec, F. Brunetti, V. Bulović, Q. Burlingame, A. Di Carlo, R. Cheacharoen, Y.-B. Cheng, A. Colsmann, S. Cros, K. Domanski, M. Dusza, C. J. Fell, S. R. Forrest, Y. Galagan, D. Di Girolamo, M. Grätzel, A. Hagfeldt, E. von Hauff, H. Hoppe, J. Kettle, H. Köbler, M. S. Leite, S. (Frank) Liu, Y.-L. Loo, J. M. Luther, C. Q. Ma, M. Madsen, M. Manceau, M. Matheron, M. McGehee, R. Meitzner, M. K. Nazeeruddin, A. F. Nogueira, Ç. Odabaşı, A. Osherov, N.-G. Park, M. O. Reese, F. De Rossi, M. Saliba, U. S. Schubert, H. J. Snaith, S. D. Stranks, W. Tress, P. A. Troshin, V. Turkovic, S. Veenstra, I. Visoly-Fisher, A. Walsh, T. Watson, H. Xie, R. Yıldırım, S. M. Zakeeruddin, K. Zhu and M. Lira-Cantu, *Nat. Energy*, 2020, **5**, 35–49.
- 3 O. V. Dolomanov, L. J. Bourhis, R. J. Gildea, J. A. K. Howard and H. Puschmann, *J. Appl. Crystallogr.*, 2009, **42**, 339–341.
- 4 G. M. Sheldrick, *Acta Crystallogr.*, 2015, **A71**, 3–8.
- 5 G. M. Sheldrick, *Acta Crystallogr.*, 2015, **C71**, 3–8.
- 6 N. T. Johnson, P. G. Waddell, W. Clegg and M. R. Probert, *Crystals*, 2017, **7**, 360.
- 7 G. M. Sheldrick, *Acta Crystallogr.*, 2008, **A64**, 112–122.
- 8 M. R. Maciejczyk, S. Zhang, G. J. Hedley, N. Robertson, I. D. W. Samuel and M. Pietraszkiewicz, *Adv. Funct. Mater.*, 2018, **1807572**, 1–13.
- 9 M. Maciejczyk, A. Ivaturi and N. Robertson, *J. Mater. Chem. A*, 2016, **4**, 4855–4863.
- 10 Ossila products page - SpiroOMeTAD, <https://www.ossila.com/products/spiro-ometad?variant=23115455681>, (accessed 7 January 2023).